

A Simple X-Ray Focusing Mirror Using Float Glass

Z. Yin* L. Berman* S. Dierker† E. Dufresne† D.P. Siddons*

ABSTRACT

In our recent x-ray photon correlation spectroscopy (speckle) experiments at NSLS, one of the challenges is to increase the coherent photon flux through a pinhole, whose size is chosen to match the beam's horizontal transverse coherence length l_h . We adopted an approach to vertically focus the x-ray beam so as to match its vertical transverse coherence length l_v (at NSLS X13, $l_v \sim 50l_h$, $l_h \sim 12 \mu\text{m}$ at 3 KeV) with l_h . By demagnifying the vertical size by a factor of l_v/l_h , we expect to increase the intensity of the x-rays through the pin hole by the same factor while keeping the beam coherent.

A piece of commercial 3/8" thick float glass, by virtue of its low surface roughness ($\sim 3\text{\AA}$ rms), good reflectivity in the low photon energy range of interest and low cost, was chosen as the mirror material. A computer controlled motorized bender with a four point bending mechanism was designed and built to bend the float glass to a continuously variable radius of curvature from -700m (intrinsic curvature of the glass surface) to $< 300\text{m}$, measured with the Long Trace Profiler at the BNL Metrology Lab. This mirror bender assembly allows us to continuously change the focal length of the x-ray mirror down to 0.5 m under our experimental conditions.

At the NSLS X13 Prototype Small Gap Undulator (PSGU) beamline, we were able to focus the x-ray beam from a vertical size of 0.5 mm to $\sim 25 \mu\text{m}$ at the focal point 54 cm from the mirror center, thus increasing the photon flux density by a factor of 20. Results also show that, as expected, at an incident angle of 9 mrad, the mirror cuts off the harmonics of the undulator spectrum, leaving a clean 3 KeV fundamental for our experiments.

1 INTRODUCTION

Interference between coherent photons scattered by random structures in a material results in a speckle pattern. The study of structure dynamics, by studying how the speckle pattern fluctuates with time, is the field of Photon Correlation Spectroscopy (PCS). Extending PCS to the x-ray region (thus, XPCS) allows one to study the material's low frequency dynamics down to interatomic spacings, and to study the opaque materials, which is not possible with visible light^{1,2}

The challenge to XPCS is that the coherent flux for x-rays is very low. In fact, XPCS work was essentially proven to be impractical until the advent of synchrotron radiation and particularly, synchrotron insertion devices, which have significantly higher brightness than bending magnet sources.

The degree of coherence of an x-ray beam can be specified by its longitudinal and transverse coherence

*National Synchrotron Light Source, Brookhaven National Laboratory, Upton, NY. 11973

†Department of Physics, University of Michigan, Ann Arbor, MI. 48109

lengths. The longitudinal coherence length, given by $\lambda^2/2\delta\lambda$, where λ is the wavelength and $\delta\lambda$ is the bandwidth, is determined by the monochromating element in the beamline. For undulator radiation, the fundamental roughly has a relative bandwidth $\delta\lambda/\lambda \sim 1/N$, where N is the number of periods of the undulator. For the Prototype Small Gap Undulator (PSGU)³ at the National Synchrotron Light Source (NSLS) X13 beamline, $N = 20$, thus, $\delta\lambda/\lambda \sim 0.05$, giving longitudinal coherence length $\lambda^2/2\delta\lambda \sim 40\text{\AA}$, if only the fundamental is chosen for the XPCS experiments. A mirror can be used to suppress the harmonics to allow only the fundamental for experiments.

The transverse coherence length of a source of horizontal and vertical size σ_h and σ_v , is given by $l_h = (\lambda/2\sigma_h)R$ and $l_v = (\lambda/2\sigma_v)R$, where R is the distance from the source. The parameters for NSLS X13 PSGU beamline are shown in Table 1. A laterally coherent beam is usually prepared by passing the x-ray beam through a pinhole with diameter equal to or less than l_h . Thus, from Table 1, much of the vertical coherent flux is not utilized.

Table 1: Transverse coherence properties of the x-ray beam at NSLS X13 PSGU. The brightness unit is ph/sec/0.1%bw/250mA/mrad².

Energy	Wavelength	σ_h	σ_v	R	l_h	l_v	Brightness
3.1KeV	4Å	414μm	8.6μm	25m	12μm	595μm	1.3×10^{17}

Better utilization of the vertical coherence length is a major challenge. We adopted an approach to vertically focus the x-ray beam, damagnifying it by a factor of l_v/l_h . One can also view this focusing as to make the vertical size of the source (virtual source) equal to the horizontal source size, making the transverse coherence length in both directions the same.

2 MIRROR DESIGN

In order for the mirror to have a good reflectivity, a smooth surface is essential. Float glass is well known for its low surface roughness ($\sim 3\text{\AA}$ rms) and good reflectivity.⁴ With its low cost and ready availability, it is the material of choice for our prototyping experiment. The dimension of the float glass used is 3/8" (thick) \times 20" (Long) \times 2" (wide).

The surface profiles of the float glass were examined by the Long Trace Profiler⁵ at Brookhaven National Laboratory (BNL). Fig.1 shows two surface profiles corresponding to two different bending torques applied.

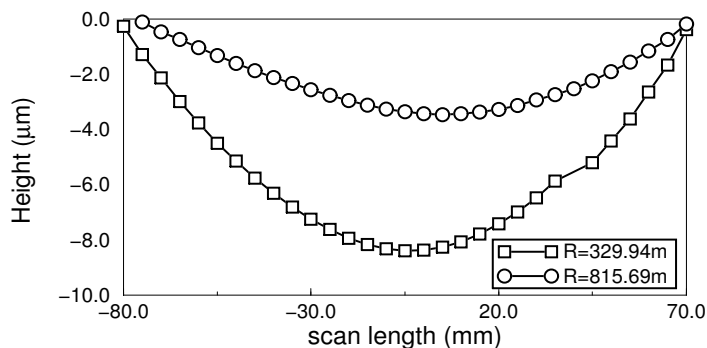


Figure 1: Example surface profiles of the float glass

A bender with a four point bending mechanism was designed to bend the float glass to approximately a cylindrical shape. Since the mirror is used in the helium environment in the x-ray experimental station X13, motorized bending is also incorporated into the design. See Fig.2 for a schematic.

Based on Fig.1, in order for the glass to be bent to a radius of curvature of, say, 300m, a displacement of only $\sim 5\mu\text{m}$ is needed for bending blocks A and B. Considering the stepping motor (200 pulses/turn) with the $\frac{1}{24}$ thread/inch screw as shown in Fig.2, which corresponds $\sim 5\mu\text{m}/\text{pulse}$, it is clear that a direct coupling between the motor and the screw would not allow us to control the bending to the desired resolution. The solution to this involves four compression springs that are inserted between each coupling and the aluminum base. Motorized rotation compresses the springs, thus applying a downward force to the glass through the shaft on the bending block (A or B). Note that when the motor moves, the coupler will move upward. As shown in the left insert of Fig.2, the coupling is designed with a pin in the coupler driven by a slotted motor shaft, allowing relative vertical motion between the coupler and the shaft. The resolution of the control hence depends on the spring constant. The distances of CA and BD can be changed to allow larger curvature, thus, shorter focal length.

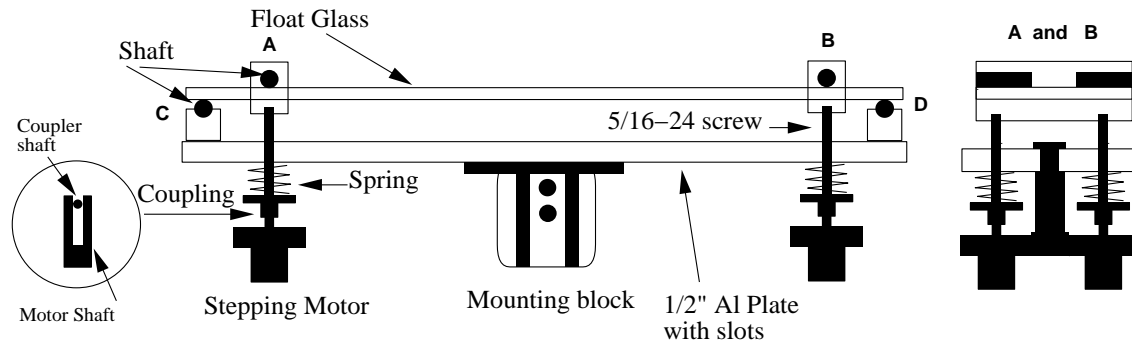


Figure 2: Schematics of the float glass mirror bender design. C and D are supports, A and B are bending blocks. All contacts to the glass are through $1/4"$ smooth steel shafts for uniform transmission of forces. The right insert shows the mirror viewed along the beam direction. Each bending block (A or B) has two motors which are fitted to a bracket that's fixed to the aluminum base.

3 EXPERIMENTAL SETUP

The experiment to test the mirror function and for XPCS is setup at the NSLS X13 beamline. The small gap undulator is operated with a gap of 7.5mm, producing undulator radiation with a fundamental of 3.1 KeV. A typical "raw" PSGU spectrum is shown in Fig.3. For our XPCS experiment, we would like to use the mirror to suppress the harmonics, therefore, monochromating the beam around the fundamental at 3.1 KeV. It is calculated that an incident angle of 9 mrad for the mirror will achieve such a result.

The mirror bender assembly is mounted on a Huber 410 rotation stage which is set on a z-translation stage. Thus a θ rotation to adjust the angle and z translation to adjust the mirror height are possible. The mirror surface is eyeballed to be coincident with the center of the rotation.

Since we are dealing with soft x-rays, we also have to cope with the x-ray absorption along the beam path. A glove box is built to contain the experimental apparatus in a helium environment and to allow experimenters to conveniently make some minor adjustments in the course of the experiment.

A CCD detector is situated 54cm from the center of the mirror to profile the beam with and without focusing. The CCD is protected by a pneumatic driven filter assembly installed along the beampath with choices of 0, 25, 50, 100, 200 μm or any of their combinations of copper foils to select the best attenuation. In order to measure the spectrum of the beam, an energy analyzer mounted on a $\theta - 2\theta$ rotation stage (Huber 414) with Si(111) analyzer crystal on the θ arm and an ion chamber on the 2θ arm can be moved into the beampath to replace the CCD detector.

All stepping motors are controlled by a computer running the NSLS ACE program through a GPIB interface to a stepping motor controller (MMC32, NSLS).

4 RESULTS

To measure the spectrum of the raw beam, the energy analyzer assembly is in place with height adjusted so that the beam hits the center on the crystal. With a $\theta - 2\theta$ scan, the energy spectrum is obtained. For the spectrum of the beam reflected off the mirror, similar measurements were performed. Fig.3 Shows a comparison of the spectrum with/without the mirror. It is clear that the mirror at 9 mrad incident angle “cuts off” the higher harmonics, leaving a clean 3.1 KeV fundamental for the XPCS experiment. With the mirror, the FWHM bandwidth of the spectrum is measured to be 200 eV, giving a longitudinal coherence length of 30\AA .

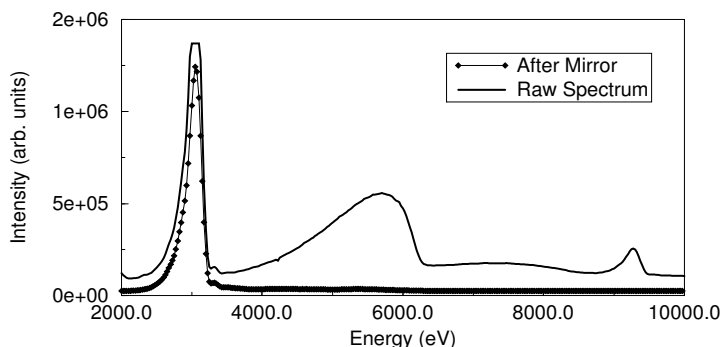


Figure 3: X13 Spectrum. The spectrum was measured with a Si(111) analyzer crystal. The spectrum after the mirror was measured with the mirror tilted at 9 mrad glancing incident angle. The flat top on the raw spectrum fundamental peak is due to saturation of the electronics. Si fluorescence excited on the Si crystal surface may be partly responsible for the differences on the two peaks and on the background level.

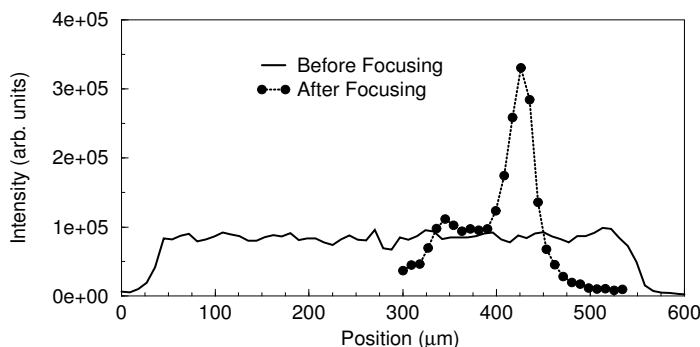


Figure 4: Vertical focusing by the float glass mirror. The mirror is tilted at 9mrad and optimum focusing is found by continuously applying torque to the mirror through the motorized mirror bender. The beam profiles are averaged over the CCD image across the horizontal direction. Note that the intensities before and after focusing are not directly comparable since the filters used in the CCD imaging are different. Because of the Cu filters, the signals detected from the CCD are from 9 KeV x-rays.

To measure the focusing ability of the mirror, the CCD detector is placed 54 cm from the center of the mirror. The primary beam is cut to $0.5\text{mm}\times 0.5\text{mm}$ by a motorized X-Y Huber slit before it enters the mirror, which is tilted to 9 mrad. The CCD is translated to find the reflected beam. The motorized mirror bender is actuated and a movie of the focused beam profile changing with bending torque is recorded. The focusing is judged by the

beam profile shown on the CCD. The beam profile of the best focus is shown as in Fig.4. It is seen that for an incident beam of 0.5 mm vertical height, it is focussed to a 25 μm vertical height.

From the beam profiles, we observed some stray-tail reflections in the vertical direction. To understand this, we performed statistical ray-tracing using the program SHADOW.⁶ Since the changing surface profile of the mirror surface is not monitored *in situ*, we use the profile that we measured before, such as in Fig.1. Fig.5 shows the resulting “image” at the nominal focal point for the bending curvature at $R = 329.94\text{m}$. The SHADOW simulation assumes a synchrotron radiation source with size $\sigma_v = 8.6\mu\text{m}$, and $\sigma_h = 414\mu\text{m}$, x-ray divergence $\sigma'_h = 260\mu\text{rad}$, $\sigma'_v = 20\mu\text{rad}$. The center of the mirror is 25m from the source, and the surface profile of Fig.1 with $R=329.94$ m is used. With a radius of curvature of 329.94 m and a source distance of 25m, the focal length is calculated to be 157.85cm.⁷ For comparison, Fig.6 shows the “image” of the beam profile for a perfect plane mirror situated at 157.85cm from the center of the mirror. From the vertical dimensions, it is clear that focusing is in effect with the bent mirror. It is also seen that stray-tail rays occur around the focal point, similar to what is observed in the experiment.

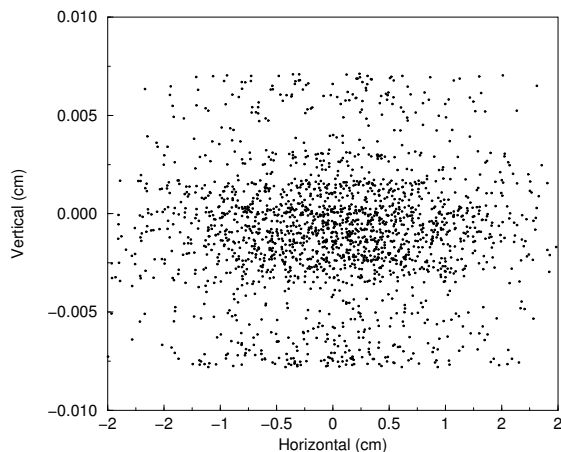


Figure 5: Curved mirror result

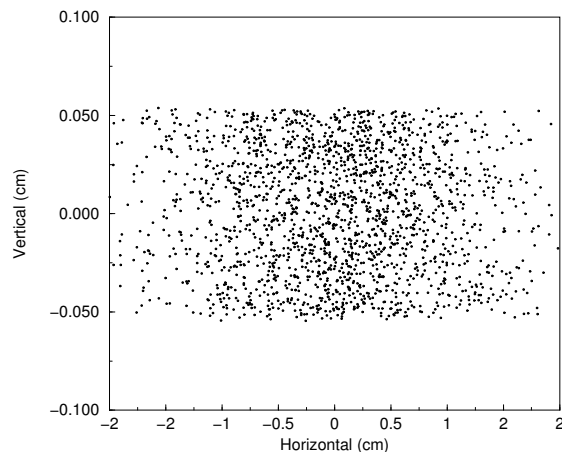


Figure 6: Plane mirror result

We believe that the stay-tail reflections are caused by aberrations of the mirror surface due to an improper figure. The spherical aberration S is given by⁸

$$S = \frac{3Mpa\alpha}{M+1} \left(\frac{M^2 + 2aM - 1}{M+1 - 2aM} \right)$$

where M is the magnification, p is the distance from the source to the mirror, $\alpha = \frac{w}{R}$, $a = \frac{\alpha}{\theta}$, w =size of the footprint, R =radius of curvature, θ =incident angle.

For $M \ll 1$, S is reduced to

$$S \simeq 3Mpa\alpha^2/\theta \simeq \frac{3w^2}{2R}$$

With the parameters used in the simulation, S is calculated to be $\sim 12\mu\text{m}$. To focus the beam to a focal length of 54cm, the mirror needs to be bent to an average radius of curvature of 117.46m. The aberration in this case is even worse ($\sim 40\mu\text{m}$, S increase inversely with R). The radius of curvature in this experiment is an order of magnitude smaller than what vertical focusing mirrors normally used because of the severe damagnification.

One way to reduce the sensitivity to the figure error is to place the mirror farther away from the pinhole (where the focus is) rather than put the mirror inside the experimental station (which is convenient). For example, if

the mirror is situated in the middle of the beamline, 13m from the source, theoretically the aberration S will be reduced to $\sim 0.8\mu\text{m}$.

Another solution is to design the mirror to bend to an true elliptical figure, not cylindrical as the present design produces. Retro-adapting this device to generate an elliptical figure is possible, by modifying the rectangular glass blank to take on an trapezoidal shape.⁹

5 CONCLUSIONS

Through our experiments, we demonstrated that commercially available float glass can be used as a mirror material in the x-ray region. By tilting the mirror to a suitable incident angle, we were able to use the mirror to cut off the unwanted higher harmonics of the undulator radiation, leaving the fundamental for our experiments. We also showed that by bending the same mirror with a motorized four-point bender, x-rays can be focussed to a demagnification factor of 20. Thus the mirror is used as a focusing mirror and a wide-bandpass "monochromator" at the same time. Unfortunately, we discovered that the current positioning of the mirror generates large aberrations that disturb the coherence of the beam. We proposed a different position for the focusing mirror, which we expect to focus the beam without disturbing the coherence, allowing us to achieve more coherent flux. Alternatively, it seems straightforward to modify this device to produce a true elliptical figure for which aberrations are minimized.

6 ACKNOWLEDGEMENTS

We would like to thank Karen Furenlid of the Optical Metrology Lab at BNL for the surface profile measurement of the float glass, Eric Johnson and Peter Stefan for support and beamline access, Tom Oversluizen for supplying the float glass blank, and Dennis Carlson and Rick Greene for their assistance on the experimental setup. The NSLS is supported by the U.S. Department of Energy under Contract No. DE-AC02-76CH00016. S. Dierker and E. Dufresne acknowledge support under NSF Grant No. DMR 92-17956.

7 REFERENCES

- [1] S. Dierker, X-Ray Photon Correlation Spectroscopy at the NSLS, NSLS newsletter, July, 1995
- [2] S. Dierker, R. Pindak, R. Fleming, I. Robinson, L. Berman, X-Ray Photon Correlation Spectroscopy Study of Brownian Motion of Colloids in Glycerol, Physical Review Letters, Vol.75, No.3, 1995, 449-452
- [3] P. Stefan, S. Krinsky, G. Rakowsky, L. Solomon, Small-Gap Undulator Experiment on the NSLS X-Ray Ring, Proceedings of 1995 IEEE Particle and Accelerator Conference, Dallas, TX, 2435. And reference therein.
- [4] D. Bilderback, S. Hubbard, X-Ray Mirror Reflections From 3.8 To 50 KeV Part I – Float Glass, Nuclear Instruments and Methods, 195, 1982, 85-89.
- [5] P. Takacs, S.K. Feng, E. Church, S. Qian, W. Liu, Long Trace Profile Measurements on Cylindrical Asphere, SPIE Proceedings, Vol. 966, 1988, 354
- [6] B. Lai, F. Cerrina, SHADOW: A Synchrotron Radiation Ray Tracing Program, Nuclear Instruments and Methods in Physics Research, A246(1986) 337-341

- [7] J. Howell, P. Horowitz, Ellipoidal and Bent Cylindrical Condensing Mirrors For Synchrotron Radiation, Nuclear Instruments and Methods, 125, 1975, 225-230
- [8] M. Howells, J. Hastings, Design Considerations For An X-Ray Microscope, Nuclear Instruments and Methods, 208, 1983, 379-386
- [9] J. Susini, X-Ray Mirrors for High Brilliance Synchrotron Beamlines R&D at the ESRF, SPIE Proceedings, Vol. 1740, 1992, 44-57